J Solid State Electrochem (2003) 7: 700–705
DOI 10.1007/s10008-003-0381-0

ORIGINAL PAPER

**M. D. Carvalho · A. Wattiaux · J. M. Bassat**
**J. C. Grenier · M. Pouchard · M. I. da Silva Pereira**
**F. M. A. Costa**

# Electrochemical oxidation and reduction of $La_4Ni_3O_{10}$ in alkaline media

Received: 26 January 2003 / Accepted: 26 March 2003 / Published online: 17 June 2003


**Abstract** In this work we used electrochemical polarization for oxidizing and reducing, in a controlled way, the Ruddlesden-Popper phase $La_4Ni_3O_{10}$. With a careful choice of electrochemical parameters, we were able to obtain samples of $La_4Ni_3O_{10\pm\delta}$ never obtained before. The oxygen stoichiometry can range between 9.78 ($\delta=-0.22$) and 10.12 ($\delta=0.12$). The oxidized phase, $La_4Ni_3O_{10.12}$, was obtained using a galvanostatic mode ($I=20$ $\mu$A) and the reduced phase, $La_4Ni_3O_{9.78}$, using potentiostatic conditions ($E=0.46$ V). The evolution of the electrical conductivity has been studied as a function of $\delta$.

**Keywords** Electrochemical oxidation · Electrochemical reduction · Oxygen intercalation · Ruddlesden-Popper phases

## Introduction

In the last few years, the electrochemical intercalation of oxygen in alkaline solution has been extensively and successfully used to control and extend the oxygen stoichiometry of oxides. The efficiency of this so-called "Chimie Douce" method was well illustrated by the electrochemical oxidation of relevant compounds such as $Sr_2M_2O_5$ (M = Fe, Co) or $La_2MO_{4+\delta}$ (M = Cu, Ni) [1, 2, 3, 4, 5, 6, 7, 8, 9, 10, 11] and by the reduction of $La_2Cu_{1-x}Ni_xO_{4+\delta}$ ($0 \le x \le 1$) compounds [11].

M. D. Carvalho (✉) · M. I. da Silva Pereira · F. M. A. Costa
Departamento de Química e Bioquímica, CCMM, F.C.U.L.,
Campo Grande C8, 1749-016 Lisbon, Portugal
E-mail: mdeus@fc.ul.pt
Tel.: +351-21-7500954
Fax: +351-21-7500088

A. Wattiaux · J. M. Bassat · J. C. Grenier · M. Pouchard
Institut de Chimie de la Matière Condensée de Bordeaux
(UPR9048/CNRS), 87 Av. Docteur A. Schweitzer,
33608 Cédex Pessac, France

Concerning compounds with the brownmillerite structure, the intercalated oxygen atoms are localized in the oxygen vacancy sites, while for the $K_2NiF_4$-type phases the location of the interstitial oxygen atoms in the $La_2O_2$ layers has been clearly demonstrated [7, 10, 12]. These studies have also shown that after the electrochemical treatment the samples remain well crystallized and oxidized/reduced in the bulk. In addition, it was demonstrated that the intercalated species are indeed the oxygen ions [2, 10, 11] and the method allows one to obtain metastable compounds.

In this work we used this electrochemical intercalation technique in order to control the oxygen stoichiometry of the $n=3$ term of $La_{n+1}Ni_nO_{3n+1\pm\delta}$ Ruddlesden-Popper phases. These compounds can be described as $n(LaNiO_3)$ perovskite blocks alternating with (LaO) rock salt layers along the crystallographic $c$ direction. The $n=1$ term of this family corresponds to $La_2NiO_4$ with the $K_2NiF_4$-type structure, while the $n=\infty$ term is the well-known $LaNiO_3$ phase with the perovskite structure.

Thus, electrochemical treatment of such compounds should be able to affect simultaneously the content of the oxygen vacancies of the perovskite $LaNiO_{3-x}$ layers, which can vary in a large way [13, 14, 15], and/or that of additional oxygen atoms inserted into the $La_2O_2$ layers of the $La_2NiO_4$-type structure, as has been demonstrated in previous work [6, 12].

The $n=3$ member of this family is particularly interesting from this point of view. During recent years, the preparation of $La_4Ni_3O_{10}$ has been reported using different synthesis methods [16, 17, 18, 19] and the obtained materials are almost oxygen stoichiometric. To our knowledge, a few over-stoichiometric phases have been mentioned, the most oxidized one being the air-prepared $La_4Ni_3O_{10.03}$, corresponding to a small over-stoichiometric value ($\delta=0.03$) [20, 21].

Conversely, some oxygen-deficient $La_4Ni_3O_{10-\delta}$ phases have been obtained after thermal treatment under a reducing atmosphere ($\delta=0.24$) [16] or during TGA

measurements using either a diluted ($\delta = 1$) [17, 22] or pure hydrogen flow ($\delta = 2$) [22]. All these phases are strongly oxygen deficient, exhibiting a tetragonal structure and semiconductor-type behaviour. We have published a report [23] highlighting the close relation between the oxygen stoichiometry and the transport properties of the $La_4Ni_3O_{10\pm\delta}$ phases.

We describe in the present work an electrochemical study of the $La_4Ni_3O_{10}$ phase in alkaline media (1 mol $L^{-1}$ KOH), which allowed us to select the electrochemical parameters for preparing the oxidized and reduced samples (anodic and cathodic polarization, respectively). The different compounds were characterized by XRD and electrical resistivity measurements before and after the electrochemical treatment.

## Experimental

Samples with nominal composition $La_4Ni_3O_{10.02}$ were prepared by a nitrate-citrate method previously described [24]. Pelleted samples of the as-prepared $La_4Ni_3O_{10.02}$ compound, with a density of about 65% (8 mm diameter, 2 mm thickness, weight ~0.4 g) were used as the working electrode. The determination of the porosity of the electrode was estimated after calculation of the density of the pellets ($\rho_{exp} = m/V$, where $m$ and $V$ represent the mass and the volume of the pellet). Then the value was compared with the crystallographic data, and the porosity was obtained by the ratio $\rho_{exp}/\rho_{cryst}$.

Electrical contact was made using a silver paste, which was separated from the electrolyte with a resin (Mecaprex KM, Presi). The electrochemical experiments were carried out using a three-electrode arrangement in a two- (cyclic voltammetry) or one- (oxidation and reduction experiments) compartment cell filled with 1 mol $L^{-1}$ KOH solution. A Hg/HgO electrode (XR400, Tacussel; $E^\circ = +0.098$ V/SHE at pH 14) was used as the reference electrode. All potentials quoted in this work are referred to this electrode. The counter electrode was a large gold foil. The experiments were performed at 25 °C in air. The electrochemical reactions (oxidation and reduction) were carried out either at steady potential (potentiostatic mode) or at constant current intensity (galvanostatic mode).

A cyclic voltammogram was first run using a rotating polished disk (rotating disk electrode EDI 101T, Tacussel, $\omega = 1000$ rpm) as the working electrode, which allowed us to determine the electrochemical conditions to be applied. This curve was obtained after stabilization at the open circuit voltage ($E_{ocv} = 0.26$ V).

After the electrochemical experiments, the pellets were removed from the cell, washed with water and acetone and then dried. The samples were characterized by powder X-ray diffraction (XRD) using a Philips PW 1730 diffractometer with Cu-$K_\alpha$ radiation after and before the electrochemical treatment. The oxidation state of nickel was determined by standard iodometric titration [25]: in the presence of an excess of potassium iodide, a mass ($m$) of the sample was dissolved in dilute HCl under nitrogen. The iodine formed was then determined by titration with a thiosulfate solution, in the presence of starch.

Electrical resistivity measurements were carried out on the pellets in the temperature range 4.2–300 K, using a standard four-probe technique.

## Results and discussion

### Voltammetry studies

A cyclic voltammogram of the $La_4Ni_3O_{10.02}$ electrode in alkaline solution is shown in Fig. 1. On the basis of this voltammogram, three oxidation ($O_i$) and three reduction ($R_i$) phenomena can be identified. As a general trend, the shape of this curve is similar to the one published for $La_2MO_{4+\delta}$ (M = Cu, Ni) phases [1, 2, 6].

It can be also noted that the cyclic voltammogram is rather similar to those previously reported for the $LaNiO_{3-\delta}$ perovskite phase [23, 24, 25, 26, 27, 28, 29], for which, before oxygen evolution, the anodic peak was associated with the redox couple $Ni^{2+}/Ni^{3+}$ [27, 28].

Considering these facts, the curve can be described as following. The linear variation (O1) of the potential, usually assigned to the double layer charging of the porous electrode, is observed in the range −0.40 to +0.40 V. The O2 process, for $0.40 < E < 0.60$ V, corresponds to the oxygen intercalation reaction into the oxide, a diffusion phenomena, described by Eq. 1:

$$La_4Ni_3O_{10}(s) + 2\delta OH^-(aq) \rightarrow La_4Ni_3O_{10+\delta}(s) + \delta H_2O(aq) + 2\delta e^- \quad (1)$$

These results are in agreement with previous work, as it was concluded that the process occurring just before the

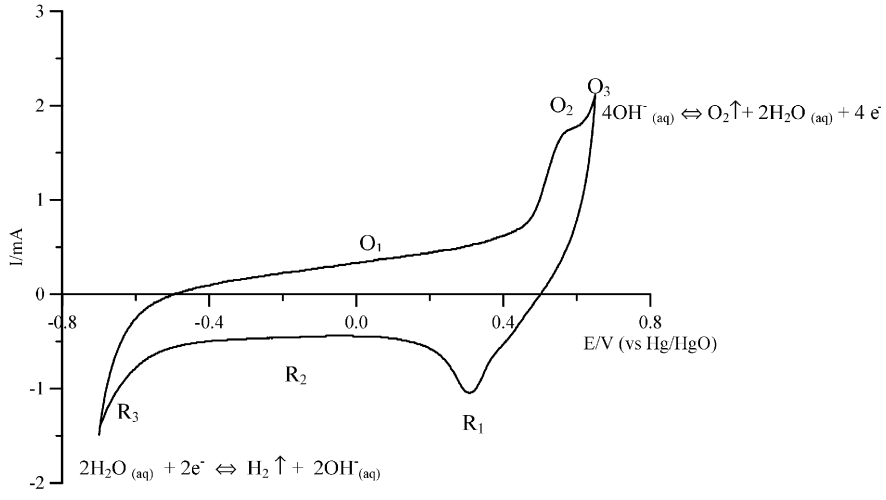


**Fig. 1** Cyclic voltammogram of the $La_4Ni_3O_{10.02}$ electrode in alkaline solution (2.5 mV/s)

oxygen evolution reaction, usually identified by a well-defined plateau, is the signature of the oxidation process of the material.

The last process (O3) appears clearly for $E > 0.60$ V, and corresponds to the oxygen evolution reaction. For $E > 0.70$ V, a gas evolution was observed on the surface electrode. However, it has to be noted that a clear separation between the O2 and O3 processes is not visible. These processes are superimposed and their deconvolution can only be carried out by a judicious choice of the electrochemical parameters. This fact is not surprising once it is known that the rate-determining step is the same for both the oxygen intercalation and oxygen evolution processes of the compound, and is described by the appearance of the $O^-$ species on the electrode surface [30, 31].

Concerning the cathodic part of the voltammogram, the peak $R_1$ around $E = 0.30$ V is likely due to the reduction of the superficial molecular oxygen absorbed during the oxidation process. The extended plateau $R_2$ ($-0.50 < E < 0.20$ V) corresponds to the reverse of Eq. 1, in agreement with previous work [10, 29], and is the signature of the reduction of the phase, by oxygen deintercalation.

A large increase of current intensity is observed for $E < -0.60$ V, which can be due to the reduction processes. This last process ($R_3$) concerns solvent reduction, with hydrogen formation, and is associated with the redox couple $H_2O/H_2$.

## Electrochemical treatment of the as-prepared samples

From the cyclic voltammetry data, the experimental conditions to perform the oxidation and reduction of the as-prepared oxide samples were selected, and are summarized in Table 1. Two polarization modes, potentiostatic and galvanostatic, were used. Concerning the first one, a steady potential of $E_{ox} = 0.46$ V ($t = 480$ h) for the oxidation process (beginning of the oxidation wave) was selected in order to avoid significant oxygen evolution. For the reduction treatment, the clear separation of the processes allowed us to choose an intermediate value of $E_{red} = -0.025$ V ($t = 480$ h) on the cathodic plateau.

Concerning the galvanostatic mode, previous studies dealing with electrochemical oxygen intercalation on oxides have shown that the current intensity should be always much smaller than those obtained by cyclic voltammetry [2, 6, 10, 32], in order to ensure that the only occurring process is the desired reaction. From these considerations, various values of the current intensity were tested (2.5, 5, 10 and 20 $\mu$A), which led us to conclude that the value of 20 $\mu$A ($t = 300$ h) appeared to be the best one to optimize the oxygen intercalation of the as-prepared compound. It is noteworthy that such a value was previously used for the electrochemical oxidation of the $La_2CuO_{4+\delta}$ phases [32]. Attempts were carried out to reduce the oxide samples using current intensities of $I = -150$ μA and $I = -100$ μA. No results of these experiments are presented, owing to the degradation signs presented by the reduced samples after the electrochemical treatment. Attempts with lower current intensities could be considered, but they would demand times of polarization much longer, which could involve chemical degradation.

**Table 1** Experimental conditions for the different electrochemical treatments

| | Oxidation conditions | Reduction conditions | |
|---|---|---|---|
| O1<br>O2 | $I = 20$ $\mu$A; 300 h<br>$E = 0.46$ V; 480 h | $E = -0.025$ V; 480 h | R |

In the case of the potentiostatic mode, when plotting the current intensity dependence with time polarization, it should be possible to follow the evolution of the reaction. However, for this kind of working electrode constituted by a pellet with large porosity, capacitive phenomena have to be taken into account and the interpretation of the $I = f(t)$ curves becomes very difficult [33, 34], owing to the double layer charging in the porous electrode. In such a case, the steady state may take quite a long time: times of the order of $10–10^4$ s are indicated by Grens and Tobias [35]. Moreover, an electroactive surface variation, even small, associated with oxygen/hydrogen evolution, disturbs significantly the current intensity.

On the other hand, for the galvanostatic mode polarization, provided that the applied current intensity is small in order to consider the oxygen/hydrogen evolution to be insignificant, it is possible to follow the rate of the reaction by representing $E$ as a function of time. Moreover from Eq. 1 it is possible to calculate the content ($\delta_{el}$) of intercalated/deintercalated species quantified by the following relation:

$$\delta_{el} = \frac{M}{2mF} It \tag{2}$$

where $I$ is the current intensity (A), $t$ the polarization time (s), $M$ the molar mass of the starting compound (g) and $m$ the pellet mass (g).

Figure 2 shows the variation of the oxide electrode potential with time, and with $\delta_{el}$ under galvanostatic conditions, during the oxidation ($I_{ox} = 20$ μA). The curve can be understood by taking into account two phenomena. For $t < 150$ h, the curve describes the oxygen intercalation mechanism into the host lattice of the oxide electrode material, and can be interpreted on the basis of some kind of extension of the Nernst law, according to the Armand equation [36, 37] described in accordance with Eq. 3:

$$E = E_{ocv} + E_r + \frac{nRT}{F} \ln\left(\frac{y}{1-y}\right) \tag{3}$$

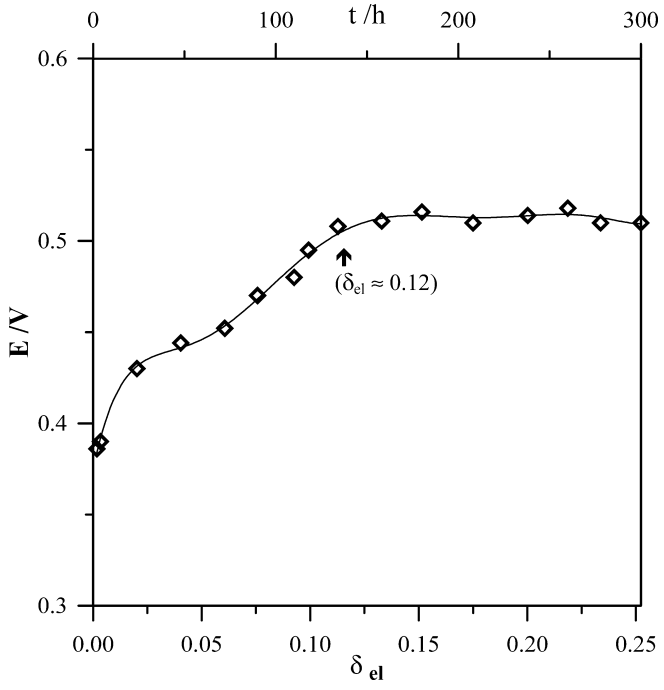


**Fig. 2** Variation of the oxide electrode potential with time and with $\delta_{el}$ under galvanostatic conditions, during the oxidation process ($I_{ox} = 20\ \mu A$)

The $E_{ocv}$ (open circuit voltage) term stands for the equilibrium potential of the working electrode in a given electrolyte. $R$, $T$ and $F$ represent respectively the gas constant, the temperature and the Faraday constant and $y$ corresponds to the fraction of occupied sites. The value of $n$ can be 1 or 2, depending on the intercalation process mechanism and $E_r$ takes into account the structure of the host lattice, the interaction effects between the intercalated species and the lattice, the diffusion path, etc. In a first approximation, for a given compound, this term should be almost constant. For $t > 150$ h, a gas evolution was observed on the electrode surface, corresponding to the oxygen evolution occurring at the electrode/electrolyte interface. So, the process is described by a simple Nernst law, the potential remains almost constant ($\sim$0.50 V) and corresponds to the equilibrium potential of the redox couple $OH^-/O_2$.

From these results and under the experimental conditions used, one can approximate the end of the intercalation of oxygen within the compound to $t = 150$ h, corresponding to $\delta = 0.12$.

## Characterization of the materials

The X-ray diffraction patterns of the two oxidized samples ($O_1$, $O_2$), as well as the reduced one, did not reveal any significant differences between them, independently of the electrochemical conditions used for the experiments. At first sight, the typical diagrams reported in Fig. 3 can be considered almost identical and it can be

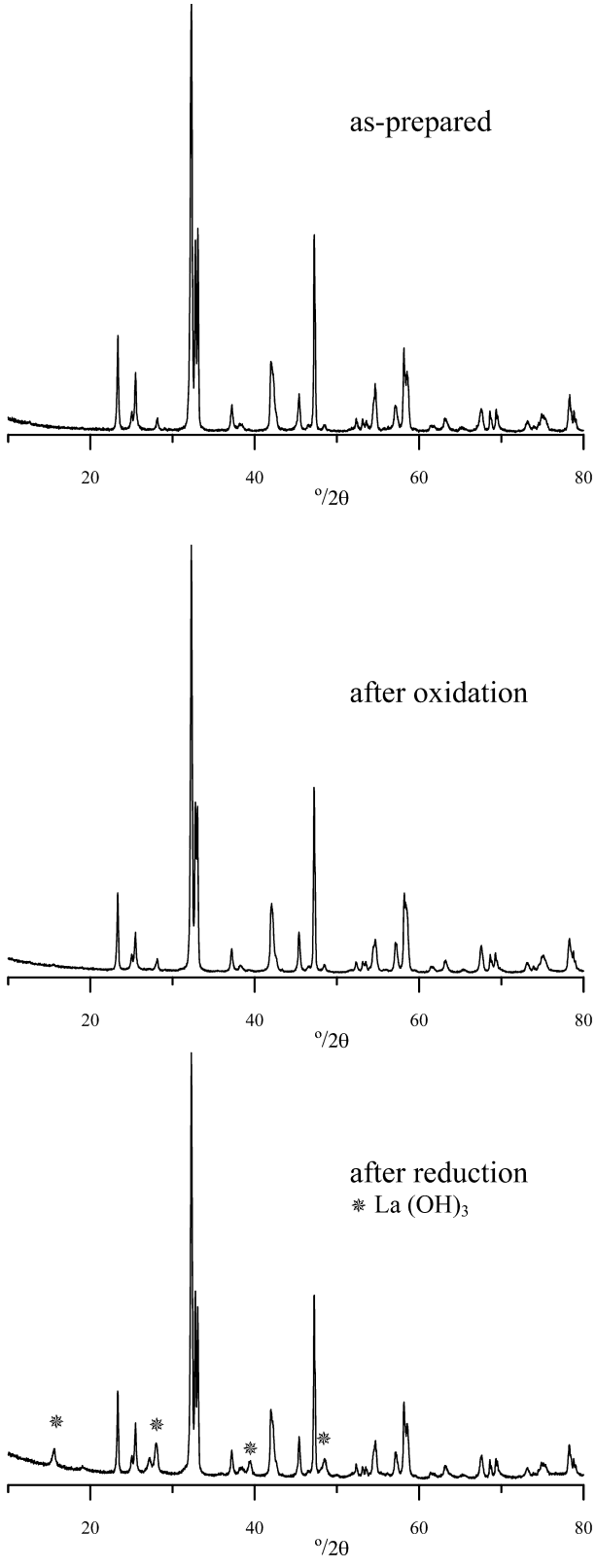


**Fig. 3** X-ray patterns of the as-prepared, oxidized and reduced compounds

**Table 2** Non-stoichiometry content calculated by iodometric titration and cell parameters of the prepared compounds

| | $\delta_{tit}$ | $Ni^{3+}$ (%) | Sample | *a* (nm) (±0.0002) | *b* (nm) (±0.0002) | *c* (nm) (±0.001) | *V* ($nm^3$) (±0.010) |
|---|---|---|---|---|---|---|---|
| As-prepared | 0.02 | 68 | $La_4Ni_3O_{10.02}$ | 0.5414 | 0.5468 | 2.796 | 0.828 |
| $O_1$ | 0.12 | 75 | $La_4Ni_3O_{10.12}$ | 0.5422 | 0.5466 | 2.796 | 0.829 |
| $O_2$ | 0.06 | 71 | $La_4Ni_3O_{10.06}$ | 0.5423 | 0.5461 | 2.796 | 0.828 |
| R[a] | −0.22 | 52 | $La_4Ni_3O_{9.78}$ | 0.5420 | 0.5469 | 2.797 | 0.829 |

[a]The small amount of $La(OH)_3$ detected in this sample was not considered in this calculation

concluded that the orthorhombic structure of the starting material is maintained after the oxidation and reduction treatments.

However, the X-ray pattern of the reduced sample exhibited some additional peaks due to the presence of $La(OH)_3$, but no traces of NiO were detected, which points to the possible formation of a soluble nickel phase. Indeed, according to the Pourbaix diagram [38], the presence of $NiOOH^-$ soluble species is possible in the conditions used in this study.

Since the amount of $La(OH)_3$ present in the reduced compounds is very small, the calculation of the oxygen non-stoichiometry ($\delta_{tit}$, determined from the chemical analysis) appears acceptable, although it is a value by default. The corresponding results of the iodometric titrations as well as the cell parameters refined for all the samples are reported in Table 2. It has to be noted that the oxygen content value calculated by this method for the sample O1 ($La_4Ni_3O_{10.12}$) is almost identical to the composition deduced from the analysis of Fig. 2, i.e. $La_4Ni_3O_{10.14}$ ($\delta_{el} = 0.12$).

Considering the values of the oxygen non-stoichiometry for the different samples studied (reported in Table 2), it is quite surprising to observe any change in the cell parameters. Actually, we expected a slight decrease of the cell parameters for the oxidized samples, as a consequence of the oxidation of $Ni^{2+}$ to $Ni^{3+}$ and, conversely, an increase of them for the reduced sample. However, considering other results on $La_2NiO_{4+\delta}$ and $La_3Ni_2O_{7-\delta}$ phases [6, 7, 22, 39], we note that an appreciable change of the cell parameters is evidenced in these Ruddlesden-Popper phases only when the deviation from the oxygen stoichiometry is meaningful. Therefore the results obtained in our work are in accordance with the rather narrow non-stoichiometry domain scanned ($-0.22 \leq \delta \leq +0.12$) with the oxygen deintercalation-intercalation processes [6, 7].

In order to check the effect of the oxygen non-stoichiometry of the samples on the transport properties, we plot in Fig. 4 the resistivity versus temperature curves for the oxidized and reduced phases, respectively. The metal-metal transition detected around 140 K for the as-prepared $La_4Ni_3O_{10.02}$ is no more perceivable for both oxidized $O_1$ and $O_2$ compounds which exhibit the same behaviour. Moreover, a slight decrease of the resistivities is observed as the oxygen content increases. For the reduced sample, a more pronounced transition is observed, as well as an increase of the resistivity values. In a recent study, we have concluded that the electrical

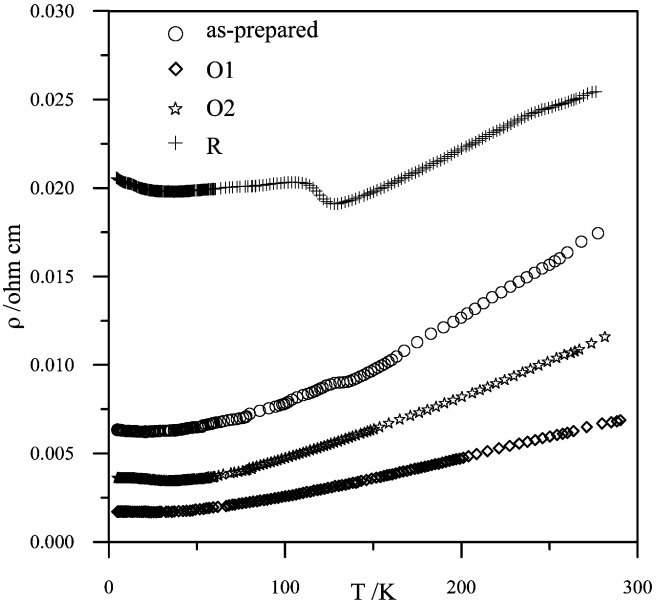


**Fig. 4** Thermal variation of the electrical resistivity of the compounds

resistivity, the Seebeck effect and the magnetic properties of these phases are closely related to their oxygen stoichiometry [23]. Slight differences in oxygen stoichiometry explain why several authors have not detected the anomaly on the electrical conductivity curve of the $La_4Ni_3O_{10}$ phase. This points to the necessity of controlling the oxygen content of these phases using electrochemical polarization, as shown in the present work.

The characterizations of the obtained $La_4Ni_3O_{10\pm\delta}$ compounds led us to conclude that under the polarization conditions used (either in oxidation or in reduction), the oxygen stoichiometry has been successfully changed. However, the presence of $La(OH)_3$ detected in the reduced sample cannot be disregarded. It clearly shows that some degradation of the surface occurred. Actually, it is quite difficult to explain simply the degradation phenomena according to the dissolution-precipitation mechanisms because of the large porosity (35%) of the electrodes.

## Conclusion

From this preliminary work we are able to conclude that electrochemical polarization is a promising method in

order to oxidize and reduce, in a controlled way, the as-prepared $La_4Ni_3O_{10.02}$ phase. It is noteworthy that there is the possibility of extending this conclusion to other Ruddlesden-Popper phases and it could also be helpful in studying the possible existence of other phases.

In these studies, we point out that the best oxidation conditions are the ones used in the galvanostatic mode ($I = 20$ μA), which permit us to obtain the $La_4Ni_3O_{10.12}$ phase. The reduction experiments allowed us to prepare the $La_4Ni_3O_{9.78}$ phase using potentiostatic conditions. However, it contains small amounts of $La_2O_3$ whatever are the polarization parameters. Different studies of the reduction conditions have to be explored in order to avoid degradation phenomena.

Recently, we have demonstrated that small changes in the oxygen stoichiometry (and consequently in the ratio $Ni^{2+}/Ni^{3+}$) play an important role in the electrical conductivity and more generally in the electronic properties of these phases [23]. It is then of great interest to control the oxygen content of the Ruddlesden-Popper phases, which can be precisely done by electrochemical polarization, as we have shown.

**Acknowledgements** The authors are grateful to Embaixada de França em Portugal and JNICT for financial support.

## References


1. Wattiaux A, Park JC, Grenier JC, Pouchard M (1990) C R Acad Sci Paris Ser II 310:1047
2. Grenier JC, Pouchard M, Wattiaux A (1996) Curr Opin Solid State Mater Sci 1:233
3. Casañ-Pastor N, Gomez-Romeiro P, Fuertes A, Navarro JM (1993) Solid State Ionics 63–65:938
4. Mahesh R, Kannan KR, Rao CNR (1995) J Solid State Chem 114:294
5. Wattiaux A, Fournés L, Zhou F, Grenier JC, Pouchard M, Etourneau J (1997) J Phys IV C1:351
6. Demourgues A, Wattiaux A, Grenier JC, Pouchard M, Soubeyroux JL, Dance JM, Hagenmuller P (1993) J Solid State Chem 105:458
7. Demourgues A, Weill F, Darriet B, Wattiaux A, Grenier JC, Gravereau P, Pouchard M (1993) J Solid State Chem 105:317
8. Bhavajaru S, Di Carlo JD, Scarfe DP, Yazdi I, Jacobson AJ (1994) Chem Mater 6:2172
9. Yazdi I, Bhavajaru S, Di Carlo JD, Scarfe DP, Jacobson AJ (1994) Chem Mater 6:2078
10. Grenier JC, Bassat JM, Doumerc JP, Etourneau J, Zhang Z, Fournes L, Petit S, Pouchard M, Wattiaux A (1999) J Mater Chem 9:25
11. Casañ-Pastor N, Zinck C, Michel CR, Tejada-Rosales EM, Torres-Gomez G (2001) Chem Mater 13:2118
12. Jorgensen JD, Dabrowski B, Shiyou Pei, Richards DR, Hinks DG (1989) Phys Rev B 40:2187
13. González-Calbet JM, Sayagués MJ, Vallet-Regí M (1989) Solid State Ionics 32:721
14. Rakshit S, Gopalakrishnan PS (1994) J Solid State Chem 110:28
15. Sayagués MJ, Vallet-Regí M, Caneiro A, González-Calbet JM (1994) J Solid State Chem 110:295
16. Kobayashi Y, Taniguchi S, Kasai M, Sato M, Nishioka T, Kontani M (1996) J Phys Soc Jpn 65:3978
17. Zhang Z, Greenblatt M (1995) J Solid State Chem 117:236
18. Mohan Ram RA, Ganapathi L, Ganguly P, Rao CNR (1986) J Solid State Chem 63:139
19. Tkalich AK, Glazkov VP, Somenkov VA, Shil'shtein S, Kar'kin AE, Mirmel'shtein AV (1991) Superconductivity 4:2280
20. Ling CD, Argyriou DN, Wu G, Neumeier JJ (1999) J Solid State Chem 152:517
21. Wu Q, Neumeier JJ, Hundley MF (2001) Phys Rev B 63:245120
22. Lacorre P (1992) J Solid State Chem 97:495
23. Carvalho MD, Cruz MM, Wattiaux A, Bassat JM, Costa FMA, Godinho M (2000) J Appl Phys 88:544
24. Carvalho MD, Costa FMA, Pereira IS, Wattiaux A, Bassat JM, Grenier JC, Pouchard M (1997) J Mater Chem 7:2107
25. Demourgues A (1992) PhD thesis. University of Bordeaux I, France
26. Matsumoto Y, Yoneyama H, Tamura H (1977) J Electroanal Chem 80:115
27. Singh RN, Jain AN, Tiwari SK, Poillerat G, Chartier P (1995) J Appl Electrochem 25:1133
28. Singh RN, Bahadur L, Pandey JP, Singh SP (1994) J Appl Electrochem 24:149
29. González M, Elizalde MP, Baños L, Poillerat G, Dávila MM (1999) Electrochim Acta 45:741
30. Wattiaux A, Grenier JC, Pouchard M, Hagenmuller P (1987) J Electrochem Soc 134:1714
31. Grenier JC, Wattiaux A, Doumerc JP, Dordor P, Fournés L, Chaminade JP, Pouchard M (1992) J Solid State Chem 96:20
32. Monroux C (1996) PhD thesis. University of Bordeaux I, France
33. Micka K (1965) Collect Czech Chem Commun 30:2288
34. Daniel-Bek VS (1946) Zh Fiz Khim 20:567
35. Grens EA, Tobias CW (1964) Z Elektrochem 68:236
36. Deportes C, Duclot M, Fabry P, Fouletier J, Hammou A, Kleitz M, Siebert E, Souquet JL (1994) Electrochimie des solides. Presses Universitaires de Grenoble, Grenoble, pp 60–61
37. Armand M, Sanchez JY, Gauthier M, Choquette Y (1994) Polymeric materials for lithium batteries. In: Lipkowski J, Ross PN (eds) Electrochemistry of novel materials. VCH, Weinheim, pp 65–69
38. Pourbaix M (1974) Atlas of electrochemical equilibria in aqueous solutions. NACE, Houston, Tex., pp 330–342
39. Zhang Z, Greenblatt M, Goodenough JB (1994) J Solid State Chem 108:402